Renewable Energy 91 (2016) 466–476

Contents lists available at ScienceDirect

Renewable Energy

journal homepage: www.elsevier.com/locate/renene

Development of a novel, robust, sustainable and low cost self-powered water pump for use in free-flowing liquid streams

D.F. Muriel [a, *], R.O. Tinoco [b], B.P. Filardo [c], E.A. Cowen [a]

[a] School of Civil and Environmental Engineering, Cornell University, Ithaca, NY 14853, USA
[b] Department of Civil and Environmental Engineering, University of Illinois at Urbana-Champaign, Urbana, IL 61801, USA
[c] Pliant Energy Systems LLC, Brooklyn, NY 11205, USA

ARTICLE INFO

Article history:
Received 28 March 2015
Received in revised form
23 January 2016
Accepted 26 January 2016
Available online 4 February 2016

Keywords:
Self-powered pumps
Hydrokinetic energy
Energy conversion
Water distribution
Water supply
Free stream flow

ABSTRACT

The design of water supply infrastructure depends on local conditions such as geophysical features, available technology, traditions, culture, and available human and economic resources. The costs for designing, building, maintaining, monitoring, and replacing the required infrastructure escalate when any of these factors is inadequate or insufficient. Furthermore, effects of global climate change increase the risk associated to existing infrastructure, calling for more robust, flexible, and adaptable technologies. We present the design and development of the first physical prototype of the Filardo Pump™, a low-cost, robust, sustainable, water-powered pump that addresses these challenges with many advantages over existing technologies: 1) it requires no external energy source, 2) it works immersed in a free-flowing, unaltered body of water, 3) it is operable in shallow water and low flow conditions, 4) it has low cost and low weight relative to work performed, and 5) it can be made small for households or scaled up for industrial applications. We show proof of concept for this novel pump and describe its development through scaling geometrical aspects and testing different materials for its operation. The proposed technology presents an opportunity for low-cost, sustainable, low carbon footprint water supplies for households, agricultural and industrial applications everywhere, not just in the rural developing world.

1. Introduction

After the Millennium Summit in 2000 and the approval of the Millennium Declaration [1], the objective of improving the water supply and sanitation sectors has played an important role in the political agenda of many countries. One of the principal goals for achieving environmental sustainability is to reduce by half the population without access to safe drinking water and sanitation by 2015. According to the United Nations [2] 11% of the global population – 783 million people – remain without access to an improved source of drinking water, and based on current trends, it is estimated that 605 million people still lacked coverage at the end of 2015. Improving coverage for rural populations is of particular concern: in 2010, 96% of the urban population had access to improved drinking water, compared with 81% of the rural population. According to the World Health Organization (WHO) and UNICEF [3] 83% of the population without access to an improved drinking water source lived in rural areas.

The disparities in the penetration of drinking water coverage between rural and urban areas clearly show that alternative approaches are required to reach more isolated or energy-poor regions. In this manuscript we present the development of the first physical prototype of a novel pump technology (invented by B. Pietro Filardo, Pliant Energy System, LLC. USA). We investigate the size and spacing of the primary pump components as well as the geometry and tuning of their support structure for efficient conversion of river kinetic energy to water lift and supplied flow rate. The presented technology is demonstrated to be robust, flexible and adaptable: it does not require an external power source, is low cost, can operate in extreme conditions (e.g. shallow water levels, debris-laden flows, or low flows), has low weight relative to work performed compared with other existing solutions, is scalable, requires little maintenance, and it can be implemented in rural areas with local materials. The Filardo Pump has the potential to transform the societal and economic conditions of a significant fraction of the population without water access by increasing quality of life,

* Corresponding author.
E-mail addresses: dfm99@cornell.edu (D.F. Muriel), tinoco@illinois.edu (R.O. Tinoco), filardo@pliantenergy.com (B.P. Filardo), eac20@cornell.edu (E.A. Cowen).

http://dx.doi.org/10.1016/j.renene.2016.01.089
0960-1481/

gender equity (in the absence of water infrastructure the labor of women represents the dominant supply of water [4,5]) and productivity of households and communities.

2. Current water lifting technologies and performance of those exploiting renewable energy sources

Water lifting mechanisms can be classified by either the water source in use, the technology implemented by the mechanism, or by the power source required to operate them [6]. Available water sources are ground water, surface water, and rain water. Water lifting technologies include: rope and bucket (loose, through a pulley, or on a windlass), bucket pump, rope pump, suction plunger hand-pump, direct action pump, deep-well piston pump, deep-well diaphragm pump, centrifugal pump, electrical submersible pump, axial flow pump, and hydraulic ram. Power sources are: human power, animal traction, wind driven, photovoltaic systems, engines (electrical, petrol, or diesel), and self- or water-powered technologies. A comprehensive description of the above mentioned technologies is reported by Fraenkel [7] and updated by Fraenkel and Thake [8]. These reviews show that despite important advancements, there is currently no technology capable of solving the water crisis in rural communities. We explore some of the disadvantages of human-, solar-, wind-, and water-powered devices below.

With respect to human powered mechanisms, Fraenkel [7] states that the costs of water-lifting human power devices is considerable and even more expensive than modern, green technologies such as solar photovoltaic panels, in addition to being plagued by maintenance problems [9]. In an attempt to address such disadvantages, variations of rope and washer pumps [10], treadle pumps [11], and flow reciprocating pumps [12] have been developed. However, such variants require special machinery and parts for maintenance and repair, affecting their sustainability and do not reduce the high costs associated with the opportunity cost of their dependance on human labor.

Solar power mechanisms suffer either from high cost per kW capacity installed, or the use of relatively sophisticated and often fragile mechanical components. First, the cost of traditional pumps powered by photovoltaic systems (PV) comes from the necessity of conversion of energy from light to electricity to mechanical force, which requires the coupling of the PV system with an existing lifting mechanism. Second, the reliability and complexity of solar thermal pumps (traditional pumps driven by closed cycle heat-engines) comes from the sophistication of the components used and solar collectors, which unfortunately are fragile. Finally, absent an energy storage device (e.g., battery) these pumps are dependent on daylight.

Wind powered mechanisms can also be divided into those powered directly by wind (i.e., mechanical energy), and those that utilize wind-generated electricity [13,14]. Regardless of the type, wind powered pumps are highly efficient in converting harvested energy into useful work, require low maintenance and can operate in a wide wind speed range. However, they have significant disadvantages that include their high initial capital cost, their size, the skills required for assembly, the intermittency of the wind resource, and their maintenance costs [15].

In the area of self-water-powered devices, waterwheels, such as the Noria, are limited in the maximum lift by their own radii while the Spiral waterwheel pump can lift water to a height several times its diameter [7,8]. For both devices the only precise machined components are the bearings and the rotating coupling that connects the pipe exiting the hub of the device to the outlet pipe for the Spiral pump. These pumps have significant disadvantages which include their initial capital cost, strong foundation requirements, and vulnerability to flood events.

Another relatively simple mechanism is the ram pump [7]. This device requires precision machined parts and a supply of water under pressure, i.e., a head differential and sealed penstock. Additionally, the coil pump and its commercial adaptation, the sling pump, operate under the same concept as self-powered devices. The coil pump is in principle an Archimedes screw operating in a horizontal plane with a coiled pipe and the sling pump adds a propeller to the design [16]. Both devices require sufficient water depth to submerge the mechanism and enough current to power them. Both designs are also limited in the maximal lift and the flow rate delivered. While a review of current patents shows a diverse range of water powered pumps, most of them require expensive machined parts [17,18].

Among the technologies presented, considerable work has gone into the application of renewable energy sources for water delivery. Gopal et al. [19] classified and reviewed different water pumping technologies based on five renewable energy categories (solar-PV, solar thermal-ST, wind, biomass, and hybrid, with no reports found for the last two).

For PV systems a wide range of applications and flow rates are found. Pande et al. [20] presented a drip irrigation system delivering 3.4–3.8 L/h against a static head of 7.1–10.2 m, Qoainder et al. [21] reported an irrigation and water supply system delivering 4.17 ML/h, and Daud and Mahmoud [22] a 2083 L/h system delivering at 37 m of head. Despite the important flow rates, Laleman et al. [23] cited several environmental impacts of such technologies, which consume large amounts of energy and emit green house gases during manufacturing, assembly, transportation, and recycling, not to mention the relative high capital costs required to procure the PV power source.

For ST systems, Sumathy et al. [24,25] report a system delivering 7.1 L/h at 10 m of head, and Wong and Sumathy [26] another one performing at 16.7–29.2 L/h at 10 and 6 m, respectively. Gopal et al. [19] listed low thermal conversion efficiency, as well as costly and unsafe working fluids among other limitations of such systems.

For wind driven systems, performances up to 3425 L/h and dynamic heads up to 50 m have been demonstrated for small capacity turbines (2.5 kW) with the downsides of mechanical and aerodynamic noise [27,28], indirect contributions to climate change [29], initial capital requirements, and impacts on animals [30].

An additional renewable energy source to consider is hydrokinetic. As with the previous sources, water supply is achieved by coupling a turbine (usually underwater) with a generator and a water pump. The key concept is that hydrokinetic devices extract the kinetic energy from the flowing water instead of potential energy from falling water [31]. Vermaak et al. [31] and Güney et al. [32] present a review of turbines and generators but no further applications for water pumping are presented. In terms of disadvantages, Vermaak et al. [31] reports high generator coupling cost due to underwater placement for horizontal axis turbines, and a starting mechanism for vertical axis turbines with low starting torque. On the other hand, Güney et al. [32] reports that the cost of generating hydrokinetic energy is strongly influenced by the power density of the stream. Also, hydrokinetic energy systems suffer similar disadvantages as wind driven systems such as high initial capital cost and environmental impacts.

2.1. The Filardo Pump

A sketch of the Filardo pump concept is shown in Fig. 1. It uses elastic materials to harness river kinetic energy to pump water. Fig. 1 (*upper left*) shows two elastic materials (hereafter called ribbons) with a membrane in the middle. By applying an external force via a tensioning element, such as tension lines, a deformation is induced within the ribbons and three pinch points (points where

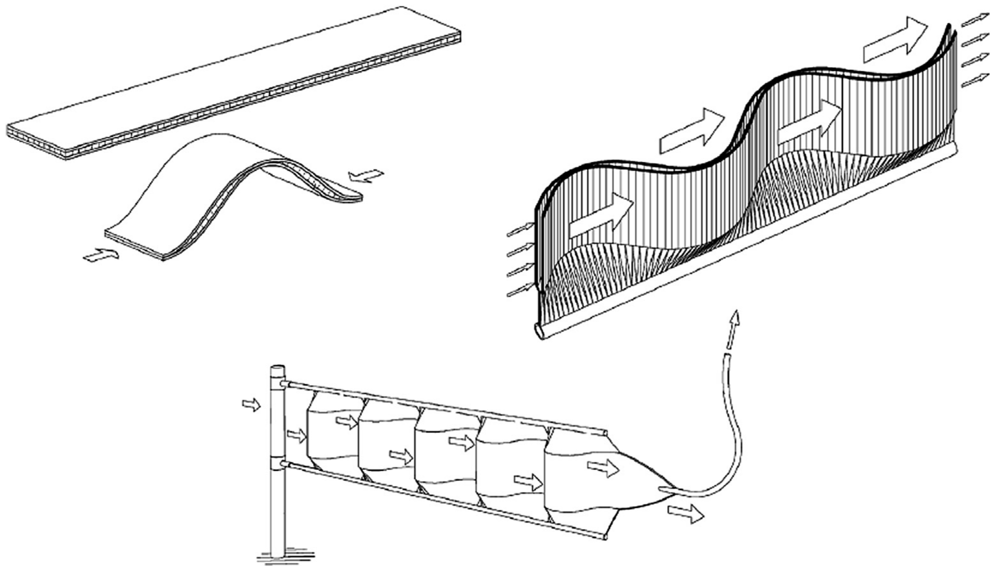

Fig. 1. The Filardo Pump concept. Elements for harnessing forces of moving fluids: elastic material coupling and deformation (*upper left*); mounting and tension lines revealed in lower half of a Filardo Pump (tension lines are lines between linear bar along bottom and sinusoidally deformed ribbon, *upper right*); general mounting for deployment (*bottom*). Drawings adapted from Filardo [33].

the two ribbons come in contact with each other in much the same way as the roller in a peristaltic pump pinches a deformable tube) are created (at the minimum and maximum points in the wave form). This external force applied is permanent and so is the deformation, locking potential energy into the system. In Fig. 1 (*upper right)* the ribbons are shown mounted and deformed by tension lines. In principle, such a deformation is permanent but unstable, allowing the ribbons to oscillate when the system is placed in moving water. As the system oscillates, the pinch points travel in the direction of the flow, and with the use of an outlet pipe and a check-valve (Fig. 1, *bottom*), water is pumped using only the energy provided by the flowing stream. A detailed description of the untested concept is presented in Filardo [33].

In summary, a number of devices have been proposed to meet the requirements of water delivery for either human use or irrigation in rural communities. Considering aspects such as robustness, cost of fabrication and installation, operation and maintenance costs, environmental impacts, among other characteristics, no single mechanism excels amongst all criteria. The Filardo Pump shows significant advantages over existing technologies (Fig. 2). Other technologies require substantial trade-offs. For example, to obtain robustness and low environmental impacts in wind, solar and thermal systems, one must be willing to support the high initial capital costs associated with minimizing these characteristics. The Filardo Pump, however, is sufficiently robust to operate under variable flow conditions with a low cost of fabrication and installation. It requires minimal maintenance and does not involve costly materials or precision machined parts.

3. Methodology

In order to demonstrate the functionality and improve performance of the pump conceptualized by Filardo [33], a series of prototypes were developed and tested varying key parameters in the Filardo Pump design. The flow rate delivered by each prototype was measured, as well as the temporal frequency of the induced

	Wind	Solar PV Electric	Solar Thermal	Noria Wheel	Sling/Spiral	Ribbon Pump	Combustion/Electric	Ram	Human/Animal
Robust	✓	-	-	×	×	✓	✓	✓	-
Very Shallow Water	✓	✓	✓	×	×	✓	✓	✓	✓
Human/animal safety	✓	✓	-	×	-	✓	-	✓	✓
Low fab cost	×	×	×	×	-	✓	×	✓	✓
Low install cost	×	✓	×	×	✓	✓	✓	×	-
Low operate/maintenance cost	-	✓	-	✓	✓	✓	×	✓	×
Low environmental cost	✓	✓	✓	✓	✓	✓	×	✓	-
Operates under surface ice	✓	✓	✓	×	×	✓	✓	-	-
24 hour operation	✓	×	×	✓	✓	✓	✓	✓	✓
Independent of weather	×	×	×	✓	✓	✓	✓	×	✓

Fig. 2. Comparison of the capabilities of various pump technologies.

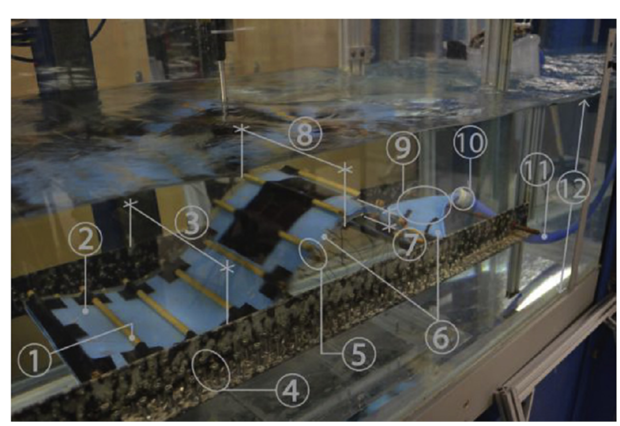

Fig. 3. Variables involved in the prototyping process: 1) transverse reinforcement, 2) thickness of the ribbons (Δ_r), 3) separation between side bars (W_r), 4) length and tension on lines, 5) internal membrane configuration and thickness (Δ_m), 6) tension lines attachment, 7) spacing between ribbons (δ), 8) width of ribbons (W), 9) outlet configuration, 10) check valve, 11) outlet pipe, and 12) water depth in the flume (H).

oscillations for each case. The variables involved in the design process are shown in Fig. 3.

3.1. Facilities and equipment

Experiments were conducted in an 8.0 *m* long, 0.60 *m* wide recirculating type open-channel flume with glass sidewalls and Super Abrasion Resistant (SAR) acrylic bed in the DeFrees Hydraulics Laboratory in the School of Civil and Environmental Engineering at Cornell University. Flows were driven by two variable frequency controlled centrifugal pumps.

Three flow depths ($H = 0.300$ *m*, $H = 0.325$ *m* and $H = 0.370$ *m*) were used, to test whether free surface effects would influence the ribbon oscillations. A Nortek Vectrino acoustic Doppler velocimeter (ADV) with Vectrino+ firmware was used for velocity measurements at different locations. The upstream mean flow velocity, U_0, was defined as the mean velocity measured on the centerline of the flume at the highest distance above the bed, where the velocity measurements were not affected by free surface effects, and located 2.0 *m* upstream from the beginning of the pump frame. The same ADV, running in distance-check mode, was used to measure amplitudes and frequencies of the ribbon oscillations. For the experiment series *T*01 to *T*03, 2^{14} samples at a rate of 200 *Hz* were taken for velocity measurements and 2^{11} samples at a rate of 10 *Hz* were collected for distance and frequency measurements in distance-check mode. For the final series (*T*04), velocity records of 2^{15} samples at 200 *Hz* were acquired. The ADV was mounted on a vernier scale allowing fine vertical adjustment, which in turn was mounted to a cart that traversed precision rails facilitating horizontal positioning.

During the early development phase of the Filardo Pump at Cornell, it became clear that a check valve at the outlet pipe was essential to increase water lift. This led immediately to the question of how significant were the energy losses through the check valves relative to the total energy of the pump. The minor loss coefficient through the check valve, $K_m = \Delta P/(\rho u^2)$, where ΔP is the pressure difference across the valve, ρ is the water density, and u is the speed of the water, were measured with a low range wet/wet differential pressure transducer (Omegadyne, Inc.). Each reported K_m is based on the mean of record lengths of 10^4 samples at 100 *Hz*.

Prototypes were tested for various operational heads, h_o, defined as the height measured from the still water surface level of the flume (± 1.5 *cm* during operation, accounting for velocity head and surface waves created by boundary effects and contact with the prototype) to the lower inner edge of the outlet pipe. Delivered flow rates were measured by collecting a volume of water over a specific period of time for all combinations of h_o and average flume speeds (U_o).

3.2. Prototypes and experiments

A number of full-scale prototypes were built in order to investigate optimal performance of the Filardo Pump. The objective was to achieve the maximum conversion of kinetic energy of the mean current to flow rate delivered at different operational heads while maintaining a simplicity in the design and affordability in terms of materials and construction, and increasing robustness. To that end, easily available materials, such as plastic gloves and diaper disposal bags, were also tested as viable materials.

For all prototypes, the ribbons are constructed from polypropylene copolymer sheets (Plastics International, MN, USA), with physical and mechanical properties available on their website or in Muriel [34] (Density: 882.3 kg/m^3, Water absorption: 0.01%, Tensile modulus: 1,52,000 *psi*). The frame side bars are made from 5.08 *cm* (2 *in*) aluminum 90° angle stock, 0.91 *m* long, with a wall thickness of 0.32 *cm* (1/8 *in*). A threaded rod, 0.79 *cm* (5/16 *in*) diameter, sets the separation between the frame side bars W_r (Fig. 3).

Microfilament braided line, 0.43 *mm* diameter, made of Spectra fiber (80 *pounds* PowerPro, Shimano American Corporation), is used for the tension lines. Separation between tension lines along the ribbon are equispaced at 2.9 *cm*, while along the frame side bars they are equispaced at 2.45 *cm*. The tension lines are tied to the edge of each ribbon, and pass through a 1 *mm* diameter hole in the frame side bars. Wire-lockable 18-8 stainless steel socket head screws (McMaster-Carr, OH, USA) are used to adjust the tension line lengths from the ribbon edges to the frame side bars (Fig. 3), providing the desired tensions and line lengths to induce the deformation in the ribbon. It is important to note that while such a configuration facilitates easy investigation of the effects of specific changes in the pump parameters, the final version for field deployment would not have as many moving, user adjustable parts.

The ribbons are mounted on a frame made of extruded aluminum alloy (McMaster-Carr, OH, USA). The frame rests on top of the flume and four legs extend into the water, allowing the ribbon pump to be set at different locations along the flume and at different elevations within the water column. The mean position of the ribbon was located 15.2 *cm* (6 *in*) above the bottom of the flume and held constant for all experimental series.

A tubular membrane (constructed from multilayer plastic films or polyethylene) was inserted between the two ribbons, leaving the upstream end open to allow for inflow. This membrane is responsible for creating the main water chambers, which are transported downstream by the pinch points as the ribbon oscillates. The membrane has a rectangular form, with the goal of covering the volume between the ribbons. The membrane terminates in a triangular shape protruding from the ribbons that connects to the water supply tube, equipped with a check valve to prevent back flow. A minor loss is introduced with this check valve and its effects were evaluated. The check valve used is taken from a CPR responder mask manufactured by Allied 100, LLC. For further details on the minor loss determination experiment see A.1.

The general objective for series *T*01 experiments was to produce the first functional prototype of the Filardo Pump. To demonstrate the oscillation and pumping capacity of two ribbons working in tandem, the parameters varied are presented in Table 1 with a detailed account of design specifications in Table 2. The internal membrane and outlet configuration can be seen on Fig. 4 (*left*).

The general objective for series *T*02 experiments was to understand the influence of the internal membrane on the flow rate delivered (*Q*). Table 1 presents the variables involved to achieve this objective, and Table 2 presents the design specifications. The internal membrane can be seen in Fig. 4 (*right*).

Series *T*03 experiments were concerned with the influence of the ribbon thickness (Δ_r) and separation (δ) on *Q*. As in previous series, the variables involved are presented in Table 1, with design specification in Table 2 and outlet configuration presented in Fig. 5 (*left*).

The final series of experiments, T04, was concerned with the influence of the ribbon width (*W*) on *Q*. The variables are presented in Table 1 and design specifications in Table 2. Also, Fig. 6 (*left*) presents the internal membrane and outlet configuration.

4. Results and discussion

In this section the four principal test series described above are discussed, some of which contain sub-series. Each successive test series was informed by questions raised in the previous series.

4.1. Series T01

As previously mentioned, this prototype series was primarily

Table 1
Objectives of prototype series *T*01 to *T*04, and *P*01.

Series	Number of prototypes	Objective	Variables involved
*T*01	10	Proof of concept	1) Transverse reinforcement 3) Separation between side bars (W_r) 4) Length and tension on lines 5) Internal membrane configuration and thickness (Δ_m) 9) Outlet configuration 10) Check valve 12) Water depth in the flume (H)
*T*02	4	Internal membrane performance	5) Internal membrane configuration and thickness (Δ_m) 9) Outlet configuration 10) Check valve 11) Outlet pipe
*P*01	8	Check valve minor loss coefficient	10) Check valve. Recirculating loop containing a pressure sensor
*T*03	4	Ribbon thickness and spacing	2) Ribbons thickness (Δ_r) 5) Internal membrane configuration and thickness (Δ_m) 6) Tension line connection 7) Spacing between ribbons (δ) 9) Outlet configuration 11) Outlet pipe
*T*04	6	Ribbon width	2) Ribbons thickness (Δ_r) 5) Internal membrane configuration and thickness (Δ_m) 8) Ribbons width (W) 9) Outlet configuration 11) Outlet pipe.

concerned with proving the ability of the two ribbons enclosing the internal membrane to pump water. The $\delta = 0.50$ *mm* ribbons ($W = 0.30$ *m*, $W_r = 0.45$ *m*, and $L = 0.60$ *m*) could not withstand the pressure build up inside the internal membrane (bladder made of $\Delta_m = 0.102$ *mm* multilayer plastic film) as the water is forced through. As seen in Fig. 6 (*right*), the ribbons deform laterally, forming a "pipe", which prevents the desired oscillations. The polypropylene sheets were reinforced transversely with four stainless steel strips and ten wood dowels, to minimize lateral deformation. Despite this transverse reinforcement, for all cases, when the outlet is constrained, either by a contraction or any fittings required to attach the exit pipe, the pressure can build up within the internal membrane, perturbing or even arresting the desired ribbon oscillations. $W_r = 0.36$ *m* (the narrowest tested), demonstrated more consistent oscillations relative to prototypes with $W_r = 0.45$ *m*, where ribbon motions often died out and required restarting by hand.

After additional wood dowels were used (20 total), the prototype with $W_r = 0.36$ *m* demonstrated consistent oscillations throughout the test and pumped water above the energy grade line (i.e., the elevation equivalent to converting all of the kinetic energy in the flowing fluid to potential energy) of the fluid in which it was immersed. The ribbon displacements in the vertical were measured using the distance-check feature of the ADV, as shown in Fig. 7, where the distance from the probe head to the ribbon surface, η (*m*), is plotted for all U_o. It is clear that the frequency of the motions increases with U_o, while the amplitude, which is set by the tension line lengths, remains essentially constant.

Oscillation frequencies are calculated from the temporal distance and velocity records. It is apparent in Fig. 8 that the frequencies of the ribbon oscillations and those of the passing vortices match for all U_o, as identified in the frequency spectra for velocity and η. Fig. 9 presents the phase velocity $c = \lambda f$, where λ is the wave length and f is the frequency of ribbon oscillations, respectively. This figure shows that there is a linear dependence between c and U_o, and that there is a minimum U_o required to start oscillations of the device and pumping (oscillations occurred below the points reported at lower U_o but no pumping was evident). This linear tendency holds for later prototypes as well.

The use of transverse reinforcement, $W_r = 0.36$ *m*, and the outlet configuration presented in Fig. 4 (*left*) provided consistent oscillations and water pumping. Fig. 10 (*a*) and Table 3 present the Q obtained for *T*01. As h_o increases Q decreases. The maximum Q at $h_o = 5$ *cm* is approximately 3.6 L/h while at $h_o = 10$ *cm* it is $Q = 1.4$ L/h. The series *T*01 prototype evinced constant leakage from the internal membrane which degraded performance, and was the primary problem targeted in series *T*02.

4.2. Series T02

The primary objective of Series *T*02 prototype was to increase Q by reducing the leakage caused by a weak internal membrane and outlet seal. Fig. 10 (*b*) reveals that by simply changing the membrane material from the diaper bag to the veterinary glove (Fig. 4, *right*), the pump performance improved. The veterinary glove provided an easy way to attach the outlet pipe and thus formed a more reliable configuration with a better seal. For *T*02 the maximum Q was 13.2 L/h while for *T*01 it was $Q = 3.6$ L/h. The internal membrane did not cover the entire width of the ribbon, reducing the water volume being acted upon by the ribbon. Series *T*03 attempted to correct this by increasing the area covered with a customized membrane.

The change in the internal membrane and the resultant flow rate increase clearly demonstrates its importance. In addition to the relevance of internal membrane robustness and size, the tension lines creating the deformation progressively tore off the plastic ribbons during tests *T*01–*T*02 and affected the performance throughout these tests. The tension induced, combined with the constant oscillation of the device, required reinforcement in the connection points between the ribbons and the tension lines. In later experiments (*T*03 and *T*04) the performance was improved by reinforcing these connection points with metal grommets.

4.3. Series P01

The goal of Series *P*01 was to understand the performance of the check valve before proceeding with further changes in the prototype. Fig. 11 shows that for the operational ranges of the pump the minimum minor loss coefficient, K_m, is 6.2 for $Q = 30$ L/h and $Re = 756$ ($Re = 4Q/\pi d\nu$, where d is the inner diameter of the outlet